

## REDUCING THE MAST VIBRATION OF SINGLE-MAST STACKER CRANES BY GAIN-SCHEDULED CONTROL

SÁNDOR HAJDU <sup>a,\*</sup>, PÉTER GÁSPÁR <sup>b</sup>

<sup>a</sup>Department of Mechanical Engineering  
University of Debrecen, H-4028, Ótemető u. 2–4, Debrecen, Hungary  
e-mail: hajdusandor@eng.unideb.hu

<sup>b</sup>Systems and Control Laboratory, Institute for Computer Science and Control  
Hungarian Academy of Sciences, H-1111, Kende u. 13–17, Budapest, Hungary  
e-mail: gaspar.peter@sztaki.mta.hu

In the frame structure of stacker cranes harmful mast vibrations may appear due to the inertial forces of acceleration or the braking movement phase. This effect may reduce the stability and positioning accuracy of these machines. Unfortunately, their dynamic properties also vary with the lifted load magnitude and position. The purpose of the paper is to present a controller design method which can handle the effect of a varying lifted load magnitude and position in a dynamic model and at the same time reveals good reference signal tracking and mast vibration reducing properties. A controller design case study is presented step by step from dynamic modeling through to the validation of the resulting controller. In the paper the dynamic modeling possibilities of single-mast stacker cranes are summarized. The handling of varying dynamical behavior is realized via the polytopic LPV modeling approach. Based on this modeling technique, a gain-scheduled controller design method is proposed, which is suitable for achieving the goals set. Finally, controller validation is presented by means of time domain simulations.

**Keywords:** robust control, LPV systems, gain-scheduling, stacker cranes.

### 1. Introduction

These days, the advanced stacker cranes of highly automated storage/retrieval systems (AS/RS) in warehouses must meet strict requirements, e.g., a fast working cycle and reliable, economical operation. This material-handling equipment often has more than one ton pay-load capacity with a 50 m lifting height, 250 m/min velocity and  $2\text{ m/s}^2$  acceleration in the direction of the aisle. Consequently, the dynamic load on the frame structure of these machines is very high. Due to the economical construction and low energy consumption operation of stacker cranes, the dead-weight of these machines is often reduced. The reduction in dead-weight may result in decreasing the stiffness of the frame structure. These structures are more responsive to dynamical loads; therefore, during operation, undesirable vibrations, low frequency and high amplitude mast sways may occur because of the different inertial forces. The

high amplitude mast vibrations may reduce the stability and positioning accuracy of the stacker crane and, in an extreme case, they may damage the structure.

For the above-mentioned reasons, it is necessary to reduce undesirable mast vibrations by controlling the traveling motion of the stacker crane (i.e., the motion towards the aisle of the warehouse). The reduction in these harmful mast vibrations has been a widely studied area within the dynamics of material handling machinery. For example, Heptner (1970) introduced several passive elements and vibration damper equipment. However, most publications attempt to reduce the structural vibrations by applying various closed-loop control techniques, e.g., pole placement with full state feedback (Dietzel, 1999) or fuzzy control (Fang *et al.*, 2008). In some papers, shape optimization of a prescribed motion-function (as a reference signal) or the determination of an optimal acceleration time are introduced to achieve the desired result (see Schumacher,

\*Corresponding author

1994). Bachmayer *et al.* (2008; 2009) demonstrate that the flatness based trajectory planning method is also applicable to vibration free mast positioning of stacker cranes. Feedforward control techniques, trajectory planning and filtering methods of stacker cranes can also be found in the works of Görgeš *et al.* (2009) and Staudecker *et al.* (2008). Sasaki *et al.* (2009) introduce a two-degree-of-freedom control system consisting of a feedforward controller based on an inverse system and a feedback controller suppressing the vibrations and stabilizing the crane. In the paper of Schindele and Aschemann (2014) an adaptive LQR-control method while in that by Aschemann *et al.* (2011) a robust control one are presented for flexible rack feeders.

Motion control as well as the estimation of structural vibrations during the design period of stacker cranes or dynamic investigation of an existing structure, require a dynamic model of a flexible structure. This model must be sufficiently accurate and at the same time simple to fulfill the requirements of control synthesis techniques. However, the dynamical properties, e.g., resonance frequencies, mode-shapes, etc., depend on the magnitude and position of the lifted load. The dynamic model must also take this effect into consideration. The main contribution of this paper is a linear parameter varying (LPV) modeling method applied for this purpose. In this model, the plant state space matrices are assumed to depend affinely on the time varying parameter, i.e., the lifted load position. Based on this modeling approach, a gain-scheduled controller is introduced with guaranteed  $\mathcal{H}_\infty$  performance.

The structure of the paper is as follows. In Section 2, after the introduction of single-mast stacker cranes, the dynamic modeling possibilities of these machines are summarized. The effect of varying lifted load properties is taken into consideration via the LPV method. In Section 3, the model order reduction method of dynamic models for LPV systems is presented, which is necessary to generate a proper LPV model. The controller synthesis method which generates a gain-scheduling controller with guaranteed  $\mathcal{H}_\infty$  performances is introduced in Section 4. The operation of the designed control system is illustrated through simulation examples in Section 5.

## 2. Dynamic modeling of single-mast stacker cranes

A schematic drawing of a single-mast stacker crane with its main components is shown in Fig. 1. The main structural unit of stacker cranes is the mast, which is a rectangular-shaped box-girder formed by precisely manufactured and welded steel sheets. For greater resistance to torsion and bending effects, the box-girder is reinforced inside by means of longitudinal stiffeners welded to the web-plate of the box-girder and horizontal

diaphragms placed evenly along the length of the mast. The mast is connected to the bottom frame (chassis) via bolted connection.

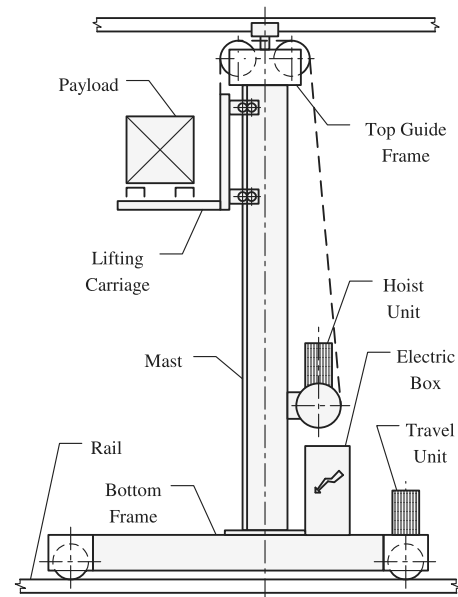


Fig. 1. Single-mast stacker crane.

The bottom frame is also a box-girder structure formed by welded steel sheets and reinforced with ribbing welded inside at regular intervals. The drive wheel and the free wheel headers are bolted to either end of the bottom frame via welded end-plates. The drive and free wheels run on the hot rolled steel rail, which is fastened to the floor of the warehouse. The purpose of the mobile lifting carriage (cradle) is to move the payload in the lifting direction and to perform the pick-up and deposit cycles with the load handling unit fitted on the carriage. The lifting carriage is a welded frame structure guided by special rollers running on the vertical guide rails of the mast.

The dynamic modeling of the single-mast stacker crane is based on the planar finite element model (FE model) shown in Fig. 2. In the model, the continuum prismatic beam sections of the mast are modeled by two-dimensional finite elements (2D beams). The other components are modeled by lumped masses, i.e., the total mass of the bottom frame (with the drive wheel and the free wheel headers, the electric box, etc.), the masses of the hoist unit and the top guide frame. The total mass of the bottom frame is denoted by  $m_{sb}$ , the mass of the hoist unit by  $m_{hd}$  and the mass of the top guide frame by  $m_{tf}$ . The effect of the lifted load, i.e., the mass of payload ( $m_p$ ) and the lifting carriage ( $m_{lc}$ ), is also taken into consideration by a lumped mass. However, the position of this lumped mass ( $h_h$ ) may vary over time and defines the lifting height. With the varying lifted load position, the

Table 1. Main parameters of the stacker crane.

Mast-height	$h_m = 45$ m
Height of hoist unit	$h_{hd} = 3.5$ m
Payload	$m_p = 1200$ kg
Mass of lifting carriage	$m_{lc} = 410$ kg
Mass of hoist unit	$m_{hd} = 470$ kg
Mass of top guide frame	$m_{tf} = 70$ kg
Mass of mast	$m_m = 5998$ kg
Mass of bottom frame	$m_{sb} = 2418$ kg

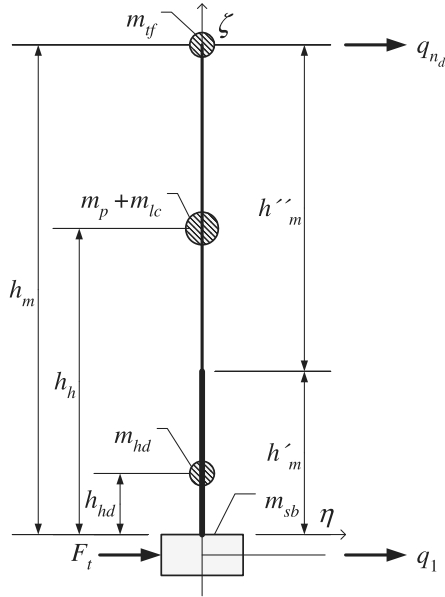


Fig. 2. Finite element model of the stacker crane.

length of finite elements surrounding the lifted load also changes. Therefore, not only the parameters but also the structure of the governing equations of motion depend on the lifting height. The main parameters of stacker crane are presented in Table 1.

The differential equation of motion of the above-mentioned finite element model can be written as

$$M\ddot{q} + K\dot{q} + Sq = u, \quad (1)$$

where  $M$  is the mass matrix,  $K$  is the damping matrix,  $S$  is the stiffness matrix,  $q = [q_1 \dots q_{n_d}]^T$  is the vector of generalized displacements,  $\dot{q}$  and  $\ddot{q}$  are the derivatives of  $q$ , i.e., the generalized velocity and acceleration vectors, and  $u$  is the vector of the external forces.

After the eigenproblem for Eqn. (1) has been solved, the eigenvectors can be arranged into the matrix  $\Phi$  with respect to the ascending order of the related natural frequencies. Using this matrix, the inverse modal transformation  $q = \Phi p$  is defined, where  $p$  is the vector of modal displacements with  $n_d$  components, and  $\Phi$  is the so-called modal matrix. Substitute the generalized displacement vector  $q$  into Eqn. (1), and then multiply

this equation by the transpose of  $\Phi$ . If the matrix  $\Phi$  is normalized to the mass matrix  $M$ , then  $\Phi^T M \Phi = I$ . In this way, the differential equation of motion (1) can be rewritten as

$$\ddot{p} + K_p \dot{p} + \Lambda p = F_p u, \quad (2)$$

where  $p$  is the vector of modal displacements,  $\dot{p}$  and  $\ddot{p}$  denote the modal velocity and acceleration vectors, respectively, and the matrices are the following:  $K_p = \Phi^T K \Phi$ ,  $\Lambda = \Phi^T S \Phi$  and  $F_p = \Phi^T$ . In the equation,  $\Lambda$  is the diagonal matrix of the squares of natural frequencies relating to the natural modes applied.

Since most control design methods use the state space representation of the model, the governing equation of motion (2) must be transformed into the state space form. The input signal of above-mentioned FE model is the external force  $u = F_t$ , i.e., the tractive force generated by the travel unit, acting on the lumped mass  $m_{sb}$  in the horizontal direction. This model is applied in the synthesis of the controller which realizes the positioning control of single-mast stacker cranes besides reduced mast vibrations.

The state space representation of a linear time invariant (LTI) system in general is described by the following equations:

$$\Sigma : \begin{cases} \dot{x} = Ax + B_1 d + B_2 u, \\ z = C_1 x + D_{11} d + D_{12} u, \\ y = C_2 x + D_{21} d, \end{cases} \quad (3)$$

where  $x$ ,  $u$ ,  $y$ ,  $d$ ,  $z$  are the state vector, control input, measured output, disturbance input and performance output vectors, respectively.

Define the state vector

$$x = [\dot{p} \ p]^T. \quad (4)$$

Using the definition above, the equations of state dynamics can be formalized as

$$\begin{bmatrix} \ddot{p} \\ \dot{p} \end{bmatrix} = \begin{bmatrix} -K_p & -\Lambda \\ I & 0 \end{bmatrix} \begin{bmatrix} \dot{p} \\ p \end{bmatrix} + \begin{bmatrix} F_p \\ 0 \end{bmatrix} u. \quad (5)$$

The first output of state space representation is denoted by  $z$  and it is the inclination of mast, i.e., the position difference between the undermost point of the mast and the mast tip  $q_1 - q_{n_d}$ . This output is used for describing and investigating mast vibrations. The second output is denoted by  $y$  and equals the horizontal position of the bottom frame, i.e., the generalized displacement  $q_1$ .

An LTI state space presentation is valid only for models with a fixed lifted load magnitude and position. However, the aim of modeling is to generate a dynamic model which is able to take the above-mentioned parameter dependence into account. Since the lifted load magnitude and position can be measured in real time, the

linear parameter varying (LPV) modeling approach has been chosen to achieve this aim. LPV systems are linear state space models whose matrices depend on the vector of time varying parameters  $\rho(t)$  (Shamma, 1988; Leith and Leithead, 2000). Hence, LPV systems are defined by state space equations as follows.

**Definition 1.** (*LPV system*) The compact set  $\mathcal{P} \subset \mathbb{R}^S$  and the continuous matrix functions  $A : \mathbb{R}^S \rightarrow \mathbb{R}^{n \times n}$ ,  $B : \mathbb{R}^S \rightarrow \mathbb{R}^{n \times n_u}$ ,  $C : \mathbb{R}^S \rightarrow \mathbb{R}^{n_y \times n}$ ,  $D : \mathbb{R}^S \rightarrow \mathbb{R}^{n_y \times n_u}$  are given. An  $n$ -th order LPV system is given by

$$\Sigma(\rho) : \begin{cases} \dot{x} = A(\rho)x + B(\rho)u, \\ y = C(\rho)x + D(\rho)u, \end{cases} \quad (6)$$

where  $\rho \in \mathcal{P}$  is the so-called scheduling parameter vector.

Unfortunately, due to the complex structure of the stacker crane mast (several kinds of sections with different cross-sectional properties, lumped masses, etc.), not only the parameters but also the form of governing equations of motion vary with the lifted load position. Another difficulty is that the large scale dynamic model with high degrees of freedom requires model order reduction before control design. Thus, it is not possible to generate the LPV model of the investigated single-mast stacker crane in one closed form. To solve this problem, a polytopic LPV modeling approach is applied (see Apkarian *et al.*, 1995). The following definitions and considerations are useful to formulate the polytopic LPV system.

**Definition 2.** (*Matrix polytope*) A matrix polytope is defined as the convex hull of a finite number of matrices  $M_i$  with the same dimensions. This convex hull can be generated as the convex combination of matrices  $M_i$ , i.e.,

$$\text{Conv} \{M_i, i = 1, \dots, n_v\} := \left\{ \sum_{i=1}^{n_v} \alpha_i M_i : \alpha_i \geq 0, \sum_{i=1}^{n_v} \alpha_i = 1 \right\}. \quad (7)$$

The investigations are restricted to such LPV systems where the state space matrices  $A(\rho)$ ,  $B(\rho)$ ,  $C(\rho)$  and  $D(\rho)$  depend affinely on the scheduling parameter vector  $\rho$  and this parameter vector varies in a polytope  $\Theta$  of vertices  $\rho_1, \rho_2, \dots, \rho_{n_v}$ , i.e.,  $\rho \in \Theta := \text{Conv} \{\rho_1, \rho_2, \dots, \rho_{n_v}\}$ . A consequence of this restriction is that the state space matrices  $A(\rho)$ ,  $B(\rho)$ ,  $C(\rho)$  and  $D(\rho)$  range in a polytope of matrices whose vertices are the images of the vertices  $\rho_1, \rho_2, \dots, \rho_{n_v}$ . That is,

$$\begin{pmatrix} A(\rho) & B(\rho) \\ C(\rho) & D(\rho) \end{pmatrix} \in \text{Conv} \left\{ \begin{pmatrix} A_i & B_i \\ C_i & D_i \end{pmatrix} := \begin{pmatrix} A(\rho_i) & B(\rho_i) \\ C(\rho_i) & D(\rho_i) \end{pmatrix}, \right. \\ \left. i = 1, \dots, n_v \right\}. \quad (8)$$

Using this property, the definition of polytopic LPV systems (see Apkarian *et al.*, 1995) can be formulated as follows.

**Definition 3.** (*Polytopic LPV system*) An LPV system is called “polytopic” when it can be represented by state space matrices  $A(\rho)$ ,  $B(\rho)$ ,  $C(\rho)$  and  $D(\rho)$ , where the parameter vector  $\rho$  ranges over a fixed polytope and the dependence of  $A(\cdot)$ ,  $B(\cdot)$ ,  $C(\cdot)$  and  $D(\cdot)$  on  $\rho$  is affine.

The main benefit of this modeling approach is that the determination of the LPV model requires the knowledge of state space matrices only in fixed vertices of the parameter space, i.e., the modeling is based on local LTI models with a “frozen” parameter vector  $\rho$ .

### 3. Model order reduction for the LPV system

As mentioned before, the aim of dynamic modeling of single-mast stacker cranes is to generate a dynamic model which is sufficiently accurate and at the same time simple to fulfill the requirements of control synthesis techniques. Due to the growth in the application of advanced modeling techniques (e.g., FE modeling), complex flexible structures, such as single-mast stacker cranes, are usually modeled by medium- or large-scale dynamic models with numerous degrees of freedom. However, applying these high-dimensional dynamic models in modern control analyses and syntheses is extremely inefficient. In most cases, the controller order is related to the order of the controlled system causing difficulties in controller realization. Modern control synthesis algorithms may also fail in controller calculation in the case of large-scale models.

Model order reduction for LPV systems is an extensively studied area with many challenges. Most of the methods introduced in the literature are based on the reduction of local LTI models of gridded LPV systems (Caigny *et al.*, 2014; Poussot-Vassal and Demourant, 2012; Poussot-Vassal and Roos, 2011; Theis *et al.*, 2015). Since the internal representation of the dynamics, i.e., the basis of the state space, at different grid points may vary due to the local reduction, an additional state transformation is required to recover state space consistency. After this transformation, the interpolation of individual LTI models can be performed in order to construct the LPV model. In this section, first the model order reduction of local LTI models is presented and after that, a similarity transformation is introduced to project the models onto the same basis. Because of the polytopic LPV modeling approach, the interpolation step can be omitted.

Since model order reduction for LTI systems is an active research field, several kinds of methods can be found in the literature (Benner *et al.*, 2003; Nowakowski

*et al.*, 2013). These methods can be grouped into three main classes:

- classical reduction methods (e.g., modal truncation),
- singular value decomposition (SVD) based methods using the controllability and observability Gramians,
- moment-matching methods based on Krylov subspaces.

The model order reduction methods listed above can be classified as projection based methods. These generate the reduced order model via projecting the original system onto a reduced one using two projection matrices whose columns form bases for relevant subspaces of the state space (see the problem below).

**Problem 1.** (*Projection based approximation*) The following LTI system with  $x \in \mathbb{R}^n$  is given:

$$\Sigma : \begin{cases} \dot{x} = Ax + Bu, \\ y = Cx + Du. \end{cases} \quad (9)$$

The aim of the projection based approximation problem is to find  $T_l \in \mathbb{R}^{r \times n}$ ,  $T_r \in \mathbb{R}^{n \times r}$  (with  $T_l T_r = I_r$ ,  $r \ll n$ ) left and right projectors such that the reduced order system  $\hat{\Sigma}$  accurately approximates  $\Sigma$ . The reduced order system  $\hat{\Sigma}$  is defined as

$$\hat{\Sigma} : \begin{cases} \dot{\hat{x}} = \hat{A}\hat{x} + \hat{B}u, \\ \hat{y} = \hat{C}\hat{x} + \hat{D}u, \end{cases} \quad (10)$$

where  $\hat{x} \in \mathbb{R}^r$ . Here the state space matrices can be calculated as  $\hat{A} = T_l A T_r$ ,  $\hat{B} = T_l B$ ,  $\hat{C} = C T_r$  and  $\hat{D} = D$ .

Projection methods differ in the way the projection matrices are chosen. Here the modal truncation (MT) method has been chosen to generate these matrices. The purpose of the MT method is to project the dynamics of the original model onto an  $A$ -invariant subspace corresponding to the dominant modes of the system. These dominant modes can be selected by the eigenvalues of  $A$ . The selection of the dominant modes plays an important role since the accuracy of approximation is determined by these modes. In the case of the investigated stacker crane model, the first two eigenvalues (with the smallest absolute values) correspond to the rigid body motion of the stacker crane, which must be retained in the reduced model. Further dominant vibrational modes (normal modes) corresponding to the next few complex conjugate eigenvalue pairs are also involved in the reduced model. In this way, the accuracy of the reduced model in the relevant frequency range will be acceptable.

As presented by Theis *et al.* (2015) in the case of LPV systems, the eigenvalues and eigenvectors of

the matrix  $A(\rho)$  are also parameter dependent and hence the transformation into a modal form would also depend on the scheduling parameter vector  $\rho$ . The use of this global parameter varying transformation introduces an explicit dependence on the parameter variation rate into the state space representation of the LPV system. This parameter variation rate dependent term may produce large off-diagonal elements in the transformed system matrix  $\hat{A}(\rho, \dot{\rho})$  for non-zero rates, which makes the decoupling impossible. Due to this problem, the above-mentioned LTI model order reduction method is applied in the fixed points of the parameter space (i.e., at the vertices  $\rho_1, \rho_2, \dots, \rho_{n_v}$  of polytope  $\Theta$  introduced in Section 2), rather than the parameter varying transformation. First a set of LTI models ( $\Sigma_i, i = 1, \dots, n_v$ ) is generated and the corresponding projector matrices  $T_{li}$  and  $T_{ri}$  are calculated. After applying these projector matrices, a set of locally reduced models ( $\hat{\Sigma}_i, i = 1, \dots, n_v$ ) is given. However, a modal state space basis calculated for an individual LTI model is not unique; therefore, the consistence of state space representations is not ensured. The physical meaning of state vector components may vary point by point. This makes it impossible to generate the polytopic LPV model from the local models. Therefore, an additional linear transformation is needed to force the states to belong to the same basis.

For this purpose, several methods can be found in the literature (see, e.g., Poussot-Vassal and Demourant, 2012; Poussot-Vassal and Roos, 2011; Theis *et al.*, 2015). From the state space projection presented in the previous section, it is known that  $x_i = T_{ri} \hat{x}_i$ . By the method introduced by Poussot-Vassal and Roos (2011) the following linear transformation is defined:  $\hat{x}_i^* = R^T x_i$ ,  $R \in \mathbb{R}^{n \times r}$ . The aim of this projection method is to force the bases of all state vectors  $\hat{x}_i^*$  to be the same. For this purpose, the linear transformation  $R$  must be generated in such a way that

$$R^T T_{r1} \hat{x}_1 = R^T T_{r2} \hat{x}_2 = \dots = R^T T_{rn_v} \hat{x}_{n_v} = \hat{x}^*. \quad (11)$$

Introducing the notation  $\hat{x}_i = Z_i^{-1} \hat{x}^*$  (where  $Z_i = R^T T_{ri}$ ), each transformed reduced-order system  $\hat{\Sigma}_i^*$  is given as

$$\hat{\Sigma}_i^* : (A_i^*, B_i^*, C_i^*, D_i^*), \quad (12)$$

where  $A_i^* = Z_i T_{li} A_i T_{ri} Z_i^{-1}$ ,  $B_i^* = Z_i T_{li} B_i$ ,  $C_i^* = C_i T_{ri} Z_i^{-1}$  and  $D_i^* = D_i$ . With the proper selection of  $R$ , the above-mentioned transformation forces the local state vectors to have the same bases, which makes the generation of polytopic LPV model possible.

The matrix  $R$  of linear transformation can be selected in several ways. It should span all the dynamics of the local models. For example, this can be the most significant transformations selected by singular value decomposition

(SVD) as follows:

$$USV^T = \text{svd}([T_{r1}, \dots, T_{rn_v}]), \quad (13)$$

where  $T_{r_i}$  denotes the local projectors corresponding to each local model. In order to keep the most significant transformations for the columns of  $R$ , the  $r$  first columns of the unitary matrix  $U$  have been chosen, i.e.,  $R = U_r$ .

The verification of the consistenc of state space bases can be performed by checking the modal trajectories (see Poussot-Vassal and Demourant, 2012), i.e., the trajectory of each eigenvalue  $\lambda_j$  with respect to the scheduling parameters  $\rho$  in the complex plane. In the case of consistent state space bases, these trajectories must have regular shapes. Another simple and intuitive idea to verify model consistenc is to inspect the regularity of the behavior of system matrix elements with respect to parameter variation.

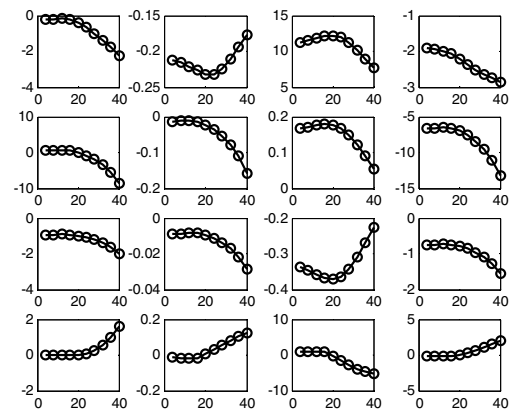
In Fig. 3, the system matrices of an example stacker crane model are analyzed and the trajectories of the system matrix elements are shown. In the example,  $D(\rho) = 0$ . The order of the reduced model is  $r = 4$ , and the numbers of input and output variables are  $n_u = 1$  and  $n_y = 2$ , respectively. The first output variable is mast inclination while the second output is the position of the stacker crane. The lifting height as scheduling parameter varies between 4 m and 44 m. From Fig. 3 it can be concluded that the matrix elements vary regularly with respect to the lifting height. Any sudden change or discontinuity cannot be seen in the functions of the matrix elements. Therefore, the consistency of dynamic models in the example of Fig. 3 is ensured point-by-point.

#### 4. LPV control design with guaranteed $\mathcal{H}_\infty$ performance

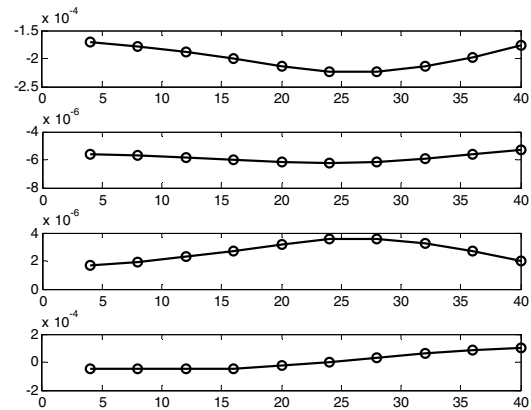
In this section, discussion of LPV control design with guaranteed  $\mathcal{H}_\infty$  performance is presented (see, e.g., Apkarian *et al.*, 1995; Packard and Balas, 1997; Bokor and Balas, 2005). Hoffmann and Werner (2015b) give a detailed summary of LPV control design methods and their application areas. Further interesting applications of LPV modeling and control can be found in the papers or Hassanabadi *et al.* (2016), Hoffmann and Werner (2015a) or Péni *et al.* (2015).

The most important tool in the formulation and derivation of the LPV controller is the *bounded real lemma* (see, e.g., Zhou *et al.*, 1996). It is originally valid for LTI systems (Gahinet and Apkarian, 1994). However, it can be extended to LPV systems using the notation of quadratic  $\mathcal{H}_\infty$  performance (see Apkarian *et al.*, 1995).

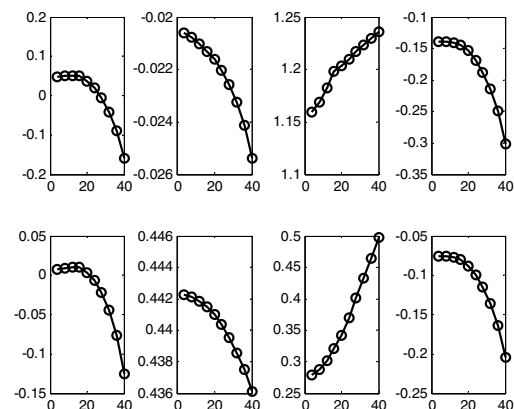
**Definition 4.** (*Quadratic  $\mathcal{H}_\infty$  performance*) The LPV system of Definition 1 has quadratic  $\mathcal{H}_\infty$  performance  $\gamma > 0$  iff there exists a symmetric matrix  $X \succ 0$  such



(a)

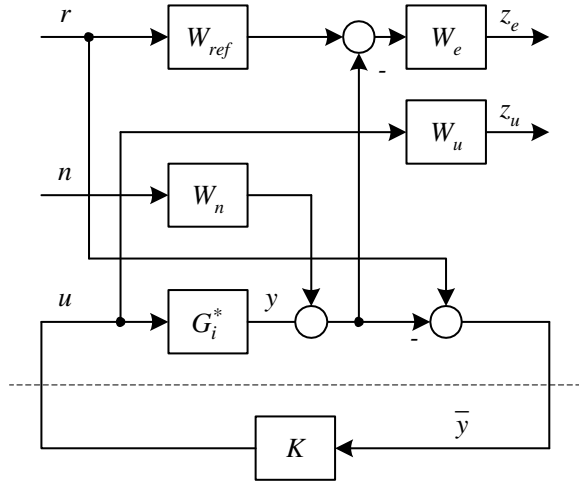


(b)



(c)

Fig. 3. Structure of system matrices:  $A(\rho)$  (a),  $B(\rho)$  (b),  $C(\rho)$  (c).


 Fig. 4.  $\mathcal{H}_\infty$  control configuration.

that

$$\begin{bmatrix} A(\rho)^T X + X A(\rho) & X B(\rho) & C(\rho)^T \\ B(\rho)^T X & -\gamma I & D(\rho)^T \\ C(\rho) & D(\rho) & -\gamma I \end{bmatrix} \prec 0 \quad (14)$$

for all admissible values of the parameter vector  $\rho$ . In this case, the Lyapunov function  $V(x) = x^T X x$  establishes global asymptotic stability and the induced  $\mathcal{L}_2$ -norm of the operator mapping from input to output is bounded by  $\gamma$  along all possible parameter trajectories  $\rho(t)$ .

Definition 4 gives an infinite number of constraints because it must be valid for all parameter vector values  $\rho \in \Theta$ . However, as shown by Apkarian *et al.* (1995) in the case of polytopic LPV systems, the infinite number of constraints can be reduced to a finite set of matrix inequalities. Due to the convexity property of the polytope, the inequality (14) will hold for all  $A(\rho)$ ,  $B(\rho)$ ,  $C(\rho)$  and  $D(\rho)$ ,  $\rho \in \Theta$ , if and only if it holds at the vertices  $(A_i, B_i, C_i, D_i)$ ,  $i = 1, \dots, n_v$ .

Before the implementation of LPV control synthesis, the control configuration for the  $\mathcal{H}_\infty$  framework, i.e., the weighting strategy of the control design, must be configured, as shown in Fig. 4. In the figure,  $G_i^*$  denotes the transfer function of the reduced order dynamic model (12) corresponding to the vertex  $\rho_i$  of polytope  $\Theta$ :

$$G(s)_i^* = C_i^* [sI - A_i^*]^{-1} B_i^*. \quad (15)$$

The mast vibration signal of dynamic model  $z$  is preserved for time domain simulation purposes. The reference signal  $r$  in the introduced augmented plant is the horizontal position demand of the stacker crane. The ideal model of the closed-loop system is represented by the transfer function  $W_{\text{ref}}$  (i.e., the so-called model matching function). Usually, this function is a second-order transfer

one with free parameters  $\omega_r$  and  $\zeta$ :

$$W_{\text{ref}} = \frac{\omega_r^2}{s^2 + 2\zeta\omega_r s + \omega_r^2}. \quad (16)$$

In this way, the bandwidth and damping of the ideal closed-loop transfer function can be adjusted. The error between the ideal and the actual closed-loop transfer functions is weighed by the penalty function  $W_e$ . The value of this penalty function should be large in a frequency range where small errors are desired and small where larger errors can be tolerated. Usually, a more accurate model is desired in the low frequency range, and therefore  $W_e$  is a low pass filter

$$W_e = \frac{A_e}{1 + T_e s}. \quad (17)$$

The control input is limited using the performance weighting function  $W_u$ . With the help of this weight, larger control signals can be penalized and thereby the control activity can be minimized. The  $W_u$  transfer function is a high pass filter with parameters  $A_u$  and  $T_u$ :

$$W_u = \frac{A_u s}{1 + T_u s}. \quad (18)$$

In general, the purpose of the weighing function  $W_n$  is to reflect sensor noise. For simplicity of calculation as well as reduction of conservatism, in the actual controller design, the setup it is omitted. Thus, the transfer function matrix of an augmented plant for control design can be expressed as

$$\begin{bmatrix} z_e \\ z_u \\ \bar{y} \end{bmatrix} = \begin{bmatrix} W_e W_{\text{ref}} & -W_e G_i^* \\ 0 & W_u \\ I & -G_i^* \end{bmatrix} \begin{bmatrix} \bar{w} \\ u \end{bmatrix}, \quad (19)$$

where  $\bar{w} = r$  is the disturbance input of the augmented plant,  $\bar{z} = [z_e \ z_u]^T$  is the vector of controlled (performance) outputs and  $\bar{y} = r - y$  is the measured output.

In this way, the controller design objective according to Definition 4 is that the induced  $\mathcal{L}_2$ -norm of the operator mapping of closed-loop system (from  $\bar{w}$  to  $\bar{z}$ ) must be bounded by  $\gamma$ , i.e.,

$$\sup_{\rho \in \Theta} \sup_{\substack{\bar{w} \in \mathcal{L}_2 \\ \|\bar{w}\|_2 \neq 0}} \frac{\|\bar{z}\|_2}{\|\bar{w}\|_2} \leq \gamma, \quad (20)$$

at the vertices  $\rho_i$  of polytope  $\Theta$ .

Taking the feedback relation  $u = K\bar{y}$  into account, the closed-loop transfer function matrix related to the vertex  $\rho_i$  of polytope  $\Theta$  can be expressed as follows:

$$\begin{aligned} M_i &= \begin{bmatrix} W_e [W_{\text{ref}} - G_i^* K (I + G_i^* K)^{-1}] \\ W_u K (I + G_i^* K)^{-1} \end{bmatrix} \\ &= \begin{bmatrix} W_e (W_{\text{ref}} - T_i) \\ W_u K S_i \end{bmatrix}, \end{aligned} \quad (21)$$

where  $S_i$  and  $T_i$  are the sensitivity and complementary sensitivity functions, respectively. Thus, the controller design objective from (20) can be formulated as

$$\|M_i\|_\infty = \left\| \begin{bmatrix} W_e(W_{\text{ref}} - T_i) \\ W_u K S_i \end{bmatrix} \right\|_\infty \leq \gamma. \quad (22)$$

It should be noted that the design objective above is similar to a mixed sensitivity loop shaping problem.

For further discussion, the state space realization of an augmented plant in vertex  $\rho_i$  is necessary, which can be constructed as follows:

$$\Sigma_{pi} : \begin{cases} \dot{\hat{x}} = A_i \bar{x} + B_{1i} \bar{w} + B_{2i} u, \\ \bar{z} = C_{1i} \bar{x} + D_{11i} \bar{w} + D_{12i} u, \\ \bar{y} = C_{2i} \bar{x} + D_{21i} \bar{w}, \end{cases} \quad (23)$$

where  $\bar{x} = [\hat{x}^T x_w^T]^T$ , with  $\hat{x}$  being the state vector of reduced order stacker crane model and  $x_w$  the state vector of weighting functions. Using (8), the polytopic LPV model of augmented plant can be written as

$$\Sigma_p(\rho) : \begin{cases} \dot{\hat{x}} = A(\rho) \bar{x} + B_1(\rho) \bar{w} + B_2(\rho) u, \\ \bar{z} = C_1(\rho) \bar{x} + D_{11}(\rho) \bar{w} + D_{12}(\rho) u, \\ \bar{y} = C_2(\rho) \bar{x} + D_{21}(\rho) \bar{w}. \end{cases} \quad (24)$$

The following assumptions for the generalized (augmented) LPV plant (24) must be made:

- (A1)  $D_{22}(\rho) = 0$  or, equivalently,  $D_{22i} = 0$  for  $i = 1, \dots, n_v$ .
- (A2)  $B_2(\rho)$ ,  $C_2(\rho)$ ,  $D_{12}(\rho)$  and  $D_{21}(\rho)$  are parameter independent or, equivalently,  $B_{2i} = B_2$ ,  $C_{2i} = C_2$ ,  $D_{12i} = D_{12}$  and  $D_{21i} = D_{21}$  for  $i = 1, \dots, n_v$ .
- (A3) The pairs  $(A(\rho), B_2)$  and  $(A(\rho), C_2)$  are quadratically stabilizable and quadratically detectable over  $\Theta$ , respectively.

Assumption (A1) can often be removed by redefining the plant output  $\bar{y}$ . If Assumption (A2) is not satisfied, the computation of a solution becomes not easily tractable. However, this problem can be solved by pre- or post-filtering of control input  $u$  or measured output  $\bar{y}$  (see Apkarian *et al.*, 1995). The third assumption is necessary and sufficient to allow quadratic stabilization of the polytopic LPV plant by an output feedback LPV controller.

The LPV controller is defined in the following way:

$$K(\rho) : \begin{cases} \dot{x}_k = A_k(\rho) x_k + B_k(\rho) \bar{y}, \\ u = C_k(\rho) x_k + D_k(\rho) \bar{y}, \end{cases} \quad (25)$$

where  $x_k \in \mathbb{R}^{n_k}$ ,  $\bar{y}$  and  $u$  are the state, input and output of the controller associated with the system (24), respectively.

As shown in Eqn. (25), since the measurements of  $\rho(t)$  are available in real time, the controller can be constructed with the same parameter dependence as the plant. Therefore the controller, can adjust to the variations in the plant dynamics in order to provide stability and performance along parameter trajectories  $\rho(t)$ . In other words, the controller is automatically gain-scheduled according to the parameter variations. Hence the closed-loop system  $\Sigma_{cl}(\rho) = \Sigma_p(\rho) * K(\rho)$  with the state vector  $x_{cl} = [\bar{x}^T x_k^T]^T$  is given by

$$\Sigma_{cl}(\rho) : \begin{cases} \dot{x}_{cl} = A_{cl}(\rho) x_{cl} + B_{cl}(\rho) \bar{d}, \\ \bar{z} = C_{cl}(\rho) x_{cl} + D_{cl}(\rho) \bar{d}, \end{cases} \quad (26)$$

where

$$\begin{aligned} A_{cl}(\rho) &= \begin{bmatrix} A(\rho) + B_2 D_k(\rho) C_2 & B_2 C_k(\rho) \\ B_k(\rho) C_2 & A_k(\rho) \end{bmatrix}, \\ B_{cl}(\rho) &= \begin{bmatrix} B_1(\rho) + B_2 D_k(\rho) D_{21} \\ B_k(\rho) D_{21} \end{bmatrix}, \\ C_{cl}(\rho) &= [C_1(\rho) + D_{12} D_k(\rho) C_2 \quad D_{21} C_k(\rho)], \\ D_{cl}(\rho) &= D_{11}(\rho) + D_{12} D_k(\rho) D_{21}. \end{aligned} \quad (27)$$

Applying (14) to (26) leads to a nonlinear (bilinear) matrix inequality, since the Lyapunov variable is multiplied by the controller variables. Via changing of the controller variables presented by Scherer *et al.* (1997), a new linear matrix inequality LMI that expresses the same problem in a tractable way can be found (cf. (29)). The decision matrices of this LMI are  $X$ ,  $Y$ ,  $\tilde{A}$ ,  $\tilde{B}$ ,  $\tilde{C}$  and  $\tilde{D}$ . Defining the matrices  $M$  and  $N$  such that  $MN^T = I_n - XY$  (which can be solved via singular value decomposition and the Cholesky factorization) the modified controller variables are (in the sequel, the parameter dependence is suppressed in the notation for simplicity):

$$\begin{aligned} \tilde{A} &= Y A X + Y B_2 D_k C_2 X + N B_k C_2 X \\ &\quad + Y B_2 C_k M^T + N A_k M^T, \\ \tilde{B} &= Y B_2 D_k + N B_k, \\ \tilde{C} &= D_k C_2 X + C_k M^T, \\ \tilde{D} &= D_k. \end{aligned} \quad (28)$$

Using these variables, the basic characterization of gain-scheduled output-feedback controllers with guaranteed  $\mathcal{H}_\infty$  performance is presented in the next theorem (for more details, see, e.g., the works of Packard and Balas (1997), Bokor and Balas (2005) or Wu (1996)).

**Theorem 1.** (Basic characterization) *The LPV plant governed by (24) is given. There exist a gain-scheduled output-feedback controller (25) enforcing internal stability and a bound  $\gamma > 0$  on the induced  $\mathcal{L}_2$ -norm of*

the closed-loop system (26) iff there exist symmetric matrices  $X$ ,  $Y$  and parameter dependent matrix variables  $(\tilde{A}, \tilde{B}, \tilde{C}, \tilde{D})$  such that for, all  $\rho \in \Theta$ , the following LMI problem holds:

$$\begin{bmatrix} M_{11} & (\bullet) & (\bullet) & (\bullet) \\ M_{21} & M_{22} & (\bullet) & (\bullet) \\ M_{31} & M_{32} & -\gamma I & (\bullet) \\ M_{41} & M_{42} & M_{43} & -\gamma I \end{bmatrix} \prec 0, \quad (29)$$

$$\begin{bmatrix} X & I \\ I & Y \end{bmatrix} \succ 0,$$

where  $\bullet$  denotes the symmetric completion of the matrix and the matrix elements are

$$\begin{aligned} M_{11} &= AX + B_2\tilde{C} + (\bullet), \\ M_{21} &= \tilde{A} + A^T + C_2^T\tilde{D}^TB_2^T, \\ M_{22} &= YA + \tilde{B}C_2 + (\bullet), \\ M_{31} &= B_1^T + D_{21}^T\tilde{D}^TB_2^T, \\ M_{32} &= B_1^TY + D_{21}^T\tilde{B}^T, \\ M_{41} &= C_1X + D_{12}\tilde{C}, \\ M_{42} &= C_1 + D_{12}\tilde{D}C_2, \\ M_{43} &= D_{11} + D_{12}\tilde{D}D_{12}. \end{aligned} \quad (30)$$

For more details and a proof of this theorem, see the works of Apkarian and Adams (1998), Chilali and Gahinet (1995), or Scherer (1995).

With no loss of generality, the LPV controller is assumed to be polytopic as well. Using the convexity property of the polytope, LPV controller synthesis can be performed via the following constructive approach:

- With the help of Theorem 1, generate and solve the LMI problem corresponding to the  $n_v$  vertices of polytope  $\Theta$  consisting of  $n_v + 1$  pieces LMIs:

$$\begin{bmatrix} M_{11i} & (\bullet) & (\bullet) & (\bullet) \\ M_{21i} & M_{22i} & (\bullet) & (\bullet) \\ M_{31i} & M_{32i} & -\gamma I & (\bullet) \\ M_{41i} & M_{42i} & M_{43i} & -\gamma I \end{bmatrix} \prec 0, \quad (31)$$

$$\begin{bmatrix} X & I \\ I & Y \end{bmatrix} \succ 0,$$

where  $i = 1, \dots, n_v$ ,  $M_{11i} = A_iX + B_{2i}\tilde{C}_i + (\bullet), \dots$ , with the notation (30).

- Using these results determine the controller system matrices  $(A_{ki}, B_{ki}, C_{ki}, D_{ki})$  at each vertex of polytope  $\Theta$  by solving the linear system (28).
- Define the LPV controller  $K(\rho)$  as the convex

combination of these vertex controllers:

$$\begin{pmatrix} A_k(\rho) & B_k(\rho) \\ C_k(\rho) & D_k(\rho) \end{pmatrix} := \left\{ \sum_{i=1}^{n_v} \alpha_i \begin{pmatrix} A_{ki} & B_{ki} \\ C_{ki} & D_{ki} \end{pmatrix} : \alpha_i \geq 0, \sum_{i=1}^{n_v} \alpha_i = 1 \right\}. \quad (32)$$

The resulting polytopic LPV controller guarantees the stability and performance of a closed loop system over the entire parameter polytope  $\Theta$ .

## 5. Mast vibration reducing LPV controller design

In this section, a design case study is presented using the modeling and controller synthesis techniques described in the previous sections. The aim of this design process is to find an adequate LPV controller which is able to handle the variations in the dynamic parameters of the stacker crane during hoisting/lowering operations. The resulting controller must provide the stability and high performance of the closed-loop system over the set of admissible parameter trajectories. Since the magnitude of the lifted load may vary only during the pick-up and deposit cycles (while the stacker crane is at a standstill), a higher level control system can adapt to this load magnitude variation by the reconfiguration of the controller. Hence, in LPV controller synthesis, only the lifted load position (lifting height) is taken into account as a scheduling variable. This reduction in the number of scheduling parameters can be very useful in the case of the polytopic LPV synthesis approach since the number of vertices grows exponentially with the number of parameters.

The dynamic model for controller synthesis and time domain simulations are generated based on the discussion presented in Section 2. Here, a 20th order FE model is used to generate the local LTI models in the vertices of the parameter polytope, i.e., both endpoints of the lifted load position. These models are reduced to the 4th order for simplicity (conserving the rigid body motion capability and first vibrational mode) and projected to the same basis via the method described in Section 3. Finally, the LPV model of the stacker crane is defined with the polytopic approach.

For defining the controller performances, the control configuration shown in Fig. 4 is used. Here, the model matching function is chosen as

$$W_{\text{ref}} = \frac{100}{s^2 + 20s + 100}. \quad (33)$$

The performance weighting functions  $W_e$  and  $W_u$  are

$$W_e = \frac{10}{1 + 10^3s}, \quad W_u = \frac{10^{-6}s}{1 + 10^{-5}s}. \quad (34)$$

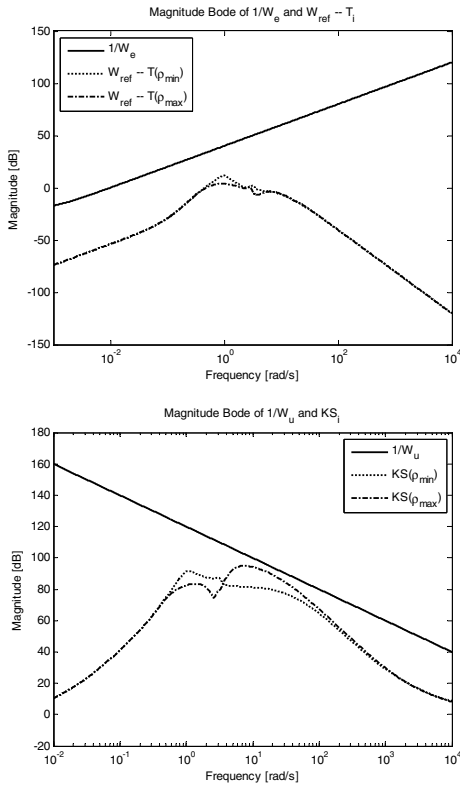


Fig. 5. Achievement of performance objectives.

Analyzing the controller design objective (22), it can be concluded that this objective implies the following conditions:

$$\begin{aligned} |W_e (W_{ref} - T_i)| &\leq \gamma, \\ |W_u K S_i| &\leq \gamma. \end{aligned} \quad (35)$$

Hence, the norms of the inverses of weighting functions  $W_e$  and  $W_u$  may be viewed as upper bounds on the transfer functions  $W_{ref} - T_i$  and  $K S_i$ , respectively. Thus the bandwidth of the closed-loop system may be affected by proper selection of the parameters of performance weighting functions. The achievement of performance objectives for the closed-loop system can be checked by means of Fig. 5.

The closed-loop system with the designed controller is tested by means of simulation based analysis. In this simulation, the position signal of a general stacker crane moving cycle is used as reference. In the first session of the moving cycle, the stacker crane has desired constant,  $0.5 \text{ m/s}^2$  acceleration. In the second session, the desired velocity is  $3.5 \text{ m/s}$  and the deceleration value of the third session is  $-0.5 \text{ m/s}^2$ . The distance covered in the moving cycle is  $70 \text{ m}$  while the total cycle time is  $27$  seconds. The lifted load position varies between  $5 \text{ m}$  and  $35 \text{ m}$  during the time-domain simulation, as shown in Fig. 6.

The simulation results, i.e., diagrams of stacker crane position  $q_1$  and mast deflection  $q_1 - q_{n_d}$ , are shown in Fig. 7.

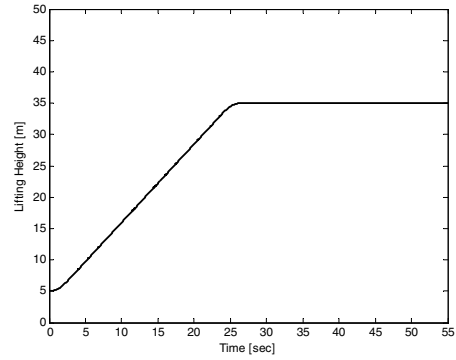
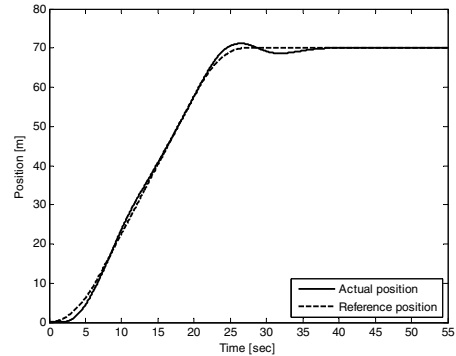
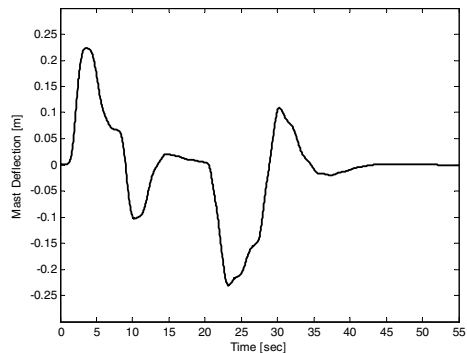


Fig. 6. Lifted load position.

For comparison purposes, the simulation diagrams generated by an LTI controller near the fixed (uppermost) load position are shown in Fig. 8. This robust LTI controller is designed with the focus on good reference signal tracking instead of reducing mast vibration.



(a)



(b)

Fig. 7. Time-domain simulation results: stacker crane position  $q_1$  (a), mast deflection  $q_1 - q_{n_d}$  (b).

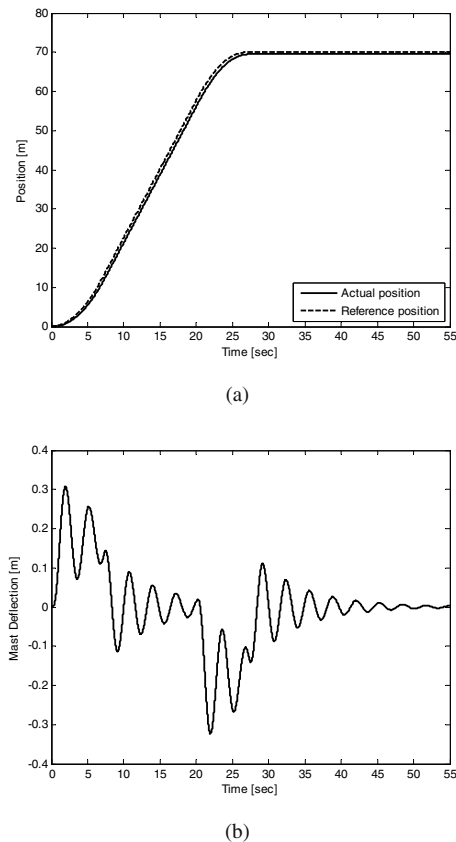


Fig. 8. Time-domain simulation results of the LTI controller: stacker crane position  $q_1$  (a), mast deflection  $q_1 - q_{nd}$  (b).

## 6. Conclusions

In the paper, a controller design method has been introduced which is able to generate a gain-scheduled controller to handle the variation in lifted load parameters during stacker crane operation. At the same time, good reference signal tracking and mast vibration reducing properties are also relevant aims of controller design. After summarizing the dynamic modeling possibilities of single-mast stacker crane structures, a local LTI model based polytopic LPV modeling approach has been presented to describe the parameter dependence of the dynamic model. Due to the relatively high-dimensional local dynamic models, first they must be reduced with a suitable method. During this model order reduction, the consistency of state space representations between parameter points is guaranteed by an additional transformation. A gain-scheduling LPV controller design method has also been introduced which is suitable for positioning control of stacker cranes with reduced mast vibrations in the presence of parameter (e.g., lifted load position) variations. The analysis of the controlled system has been carried out via time domain simulations. The

results show acceptable reference signal tracking and mast vibration reducing properties.

## References

- Apkarian, P. and Adams, R.J. (1998). Advanced gain-scheduling techniques for uncertain systems, *IEEE Transactions on Control Systems Technology* **6**(1): 21–32.
- Apkarian, P., Gahinet, P. and Becker, G. (1995). Self-scheduled  $\mathcal{H}_\infty$  control of linear parameter-varying systems: A design example, *Automatica* **31**(9): 1251–1261.
- Aschemann, H., Schindele, D. and Ritzke, J. (2011). *Modeling, Design, and Simulation of Systems with Uncertainties*, Springer, Berlin/Heidelberg, pp. 333–351.
- Bachmayer, M., Schipplick, M., Thümmel, T., Kessler, S., Ulbrich, H. and Günthner, W.A. (2008). Nachschwingungsfreie Positionierung elastischer Roboter durch numerische und analytische Trajektorienplanung am Beispiel Regalbediengerät, *VDE/VDI-Tagung: Elektrisch-mechanische Antriebssysteme—Innovationen—Trends—Mechatronik, Böblingen, Germany*, pp. 1–7.
- Bachmayer, M., Zander, R. and Ulbrich, H. (2009). Numerical approaches for residual vibration free positioning of elastic robots, *Materialwissenschaft und Werkstofftechnik* **40**(3): 161–168.
- Benner, P., Quintana-Orti, E.S. and Quintana-Orti, G. (2003). State-space truncation methods for parallel model reduction of large-scale systems, *Parallel Computing* **29**(11–12): 1701–1722.
- Bokor, J. and Balas, G. (2005). Linear parameter varying systems: A geometric theory and applications, *16th IFAC World Congress, Prague, Czech Republic*, pp. 12–22.
- Caigny, J.D., Pintelon, R., Camino, J.F. and Swevers, J. (2014). Interpolated modeling of LPV systems, *IEEE Transactions on Control Systems Technology* **22**(6): 2232–2246.
- Chilali, M. and Gahinet, P. (1995).  $\mathcal{H}_\infty$  design with pole placement constraints: An LMI approach, *IEEE Transactions on Automatic Control* **41**(3): 358–367.
- Dietzel, M. (1999). *Beeinflussung des Schwingungsverhaltens von Regalbediengeräten durch Regelung des Fahrtriebs*, dissertation, Institut für Fördertechnik Karlsruhe, Karlsruhe.
- Fang, H., Yueting, C. and Shouhua, Z. (2008). Application of fuzzy control in the stacker crane of an AS/RS, *5th International Conference on Fuzzy Systems and Knowledge Discovery, Jinan, Shandong, China*, pp. 508–512.
- Gahinet, P. and Apkarian, P. (1994). A linear matrix inequality approach to  $\mathcal{H}_\infty$  control, *International Journal of Robust and Nonlinear Control* **4**(4): 421–448.
- Görges, D., Kroneis, J. and Liu, S. (2009). Active vibration control of storage and retrieval machines, *Proceedings of the ASME 2008 International Design Engineering Technical Conferences & Computers and Information in Engineering Conference, New York, NY, USA*, pp. 1037–1046.

- Hassanabadi, A.H., Shafiee, M. and Puig, V. (2016). Robust fault detection of singular LPV systems with multiple time-varying delays, *International Journal of Applied Mathematics and Computer Science* **26**(1): 45–61, DOI: 10.1515/amcs-2016-0004.
- Heptner, K. (1970). Dynamisches Fahrverhalten von Regalförderzeugen und Dämpfung ihrer Schwingungen, *Fördern und Heben* **20**(16): 918–922.
- Hoffmann, C. and Werner, H. (2015a). LFT-LPV modeling and control of a control moment gyroscope, *54th IEEE Conference on Decision and Control (CDC), Osaka, Japan*, pp. 5328–5333.
- Hoffmann, C. and Werner, H. (2015b). A survey of linear parameter-varying control applications validated by experiments or high-fidelity simulations, *IEEE Transactions on Control Systems Technology* **23**(2): 416–433.
- Leith, D. and Leithead, W. (2000). Survey of gain-scheduling analysis and design, *International Journal of Control* **73**(11): 1001–1025.
- Nowakowski, C., Kürschner, P., Eberhard, P. and Benner, P. (2013). Model reduction of an elastic crankshaft for elastic multibody simulations, *Journal of Applied Mathematics and Mechanics* **93**(4): 198–216.
- Packard, A. and Balas, G. (1997). Theory and application of linear parameter varying control techniques, *American Control Conference, Albuquerque, NM, USA, Workshop I*.
- Péni, T., Vanek, B., Szabó, Z. and Bokor, J. (2015). Supervisory fault tolerant control of the GTM UAV using LPV methods, *International Journal of Applied Mathematics and Computer Science* **25**(1): 117–131, DOI: 10.1515/amcs-2015-0009.
- Poussot-Vassal, C. and Demourant, F. (2012). Dynamical medium (large)-scale model reduction and interpolation with application to aircraft systems, *Aerospace Lab* **4**(1): 1–11.
- Poussot-Vassal, C. and Roos, C. (2011). Flexible aircraft reduced-order LPV model generation from a set of large-scale LTI models, *Proceedings of the IEEE American Control Conference, San Francisco, CA, USA*, pp. 745–750.
- Sasaki, M., Shimizu, T., Ikai, K. and Ito, S. (2009). Two-degree-of-freedom control of a stacker crane, *ICROS-SICE International Joint Conference, Fukuoka, Japan*, pp. 874–878.
- Scherer, C. (1995). Mixed  $\mathcal{H}_2/\mathcal{H}_\infty$  control, in A. Isidori (Ed.), *Trends in Control: A European Perspective*, Springer-Verlag, London, pp. 173–216.
- Scherer, C., Gahinet, P. and Chilali, M. (1997). Multiobjective output-feedback control via LMI optimization, *IEEE Transaction on Automatic Control* **42**(7): 896–911.
- Schindele, D. and Aschemann, H. (2014). Adaptive LQR-control design and friction compensation for flexible high-speed rack feeders, *Journal of Computational and Nonlinear Dynamics* **9**(1): 1–9.
- Schumacher, M. (1994). *Untersuchung des Schwingungsverhaltens von Einmast-Regalbediengeräten*, Dissertation, Institut für Fördertechnik Karlsruhe, Karlsruhe.
- Shamma, J.S. (1988). *Analysis and Design of Gain Scheduled Control Systems*, Ph.D. thesis, Laboratory for Information and Decision Systems, Cambridge, MA.
- Stauder, M., Schlacher, K. and Hansl, R. (2008). Passivity based control and time optimal trajectory planning of a single mast stacker crane, *Proceedings of the 17th IFAC World Congress (IFAC'08), Seoul, Korea*, pp. 875–880.
- Theis, J., Takarics B., Pfifer H., Balas G. and Werner H. (2015). Modal matching for LPV model reduction of aeroservoelastic vehicles, *AIAA Atmospheric Flight Mechanics Conference, Kissimmee, FL, USA*, pp. 1–12.
- Wu, F. (1996). Induced  $\mathcal{L}_2$  norm model reduction of polytopic uncertain linear systems, *Automatica* **32**(10): 1417–1426.
- Zhou, K., Doyle, J.C. and Glover, K. (1996). *Robust and Optimal Control*, Prentice Hall, Upper Saddle River, NJ.



**Sándor Hajdu** received his M.Sc. in mechanical engineering from the Budapest University of Technology and Economics (BUTE) in 2002. Since 2008, he has been an assistant professor at the Faculty of Engineering, University of Debrecen. Presently, he is also a Ph.D. student at the Department of Control and Transport Automation, BUTE. His research interests include mechanical systems and vehicle structures.



**Péter Gáspár** received both his M.Sc. and Ph.D. degrees from the Faculty of Transportation and Vehicle Engineering, Budapest University of Technology and Economics (BUTE), in 1985 and 1997, respectively, and his D.Sc. in control from the Hungarian Academy of Sciences (HAS) in 2007. Since 1990, he has been a research advisor in the Systems and Control Laboratory (SCL), Computer and Automation Research Institute, HAS. He is the head of the Department of Control and Transport Automation, BUTE. His research interests include linear and nonlinear systems, multi-objective control, vehicle structures and control.

Received: 13 September 2015

Revised: 9 March 2016

Accepted: 10 August 2016